Phase-Space Approach to Solving the Time-Independent Schrödinger Equation

Asaf Shimshovitz and David J. Tannor

Department of Chemical Physics, Weizmann Institute of Science, Rehovot 76100, Israel

(Received 20 June 2010; revised manuscript received 13 December 2011; published 17 August 2012)

We propose a method for solving the time-independent Schrödinger equation based on the von Neumann (vN) lattice of phase space Gaussians. By incorporating periodic boundary conditions into the vN lattice [F. Dimler *et al.*, New J. Phys. **11**, 105052 (2009)], we solve a longstanding problem of convergence of the vN method. This opens the door to tailoring quantum calculations to the underlying classical phase space structure while retaining the accuracy of the Fourier grid basis. The method has the potential to provide enormous numerical savings as the dimensionality increases. In the classical limit, the method reaches the remarkable efficiency of one basis function per one eigenstate. We illustrate the method for a challenging two-dimensional potential where the Fourier grid method breaks down.

DOI: 10.1103/PhysRevLett.109.070402 PACS numbers: 03.65.Fd, 02.70.Hm, 02.70.Jn, 82.20.Wt

The formal framework for quantum mechanics is an infinite dimensional Hilbert space. In any numerical calculation, however, a wave function is represented in a finite dimensional basis set and, therefore, the choice of basis set determines the accuracy. The optimal basis set should combine accuracy and flexibility, allowing a small number of basis functions to represent the wave functions even in the presence of complex boundary conditions and geometry. Unfortunately, these two criteria—accuracy and efficiency—are usually in conflict, and globally accurate methods [1–3] lack the flexibility of local methods [4–7]. For example, in the pseudospectral Fourier grid method, the wave function is represented by its values on a finite number of evenly spaced grid points. Due to the Nyquist sampling theorem, this allows for an exact representation of the wave, provided the wave function is band-limited with finite support [8–10]. However, the nonlocal form of the basis functions in momentum space leads to limited efficiency. On the other hand, in the von Neumann basis set [11,12] each basis function is localized on a unit cell of size h in phase space. However, despite the formal completeness of the vN basis set [13], attempts to utilize this basis in quantum numerical calculations have been plagued with numerical errors [4,14].

In this Letter, we establish a precise mathematical formalism for the vN basis on a truncated phase space. By using periodic boundary conditions in the vN basis, as introduced in the seminal work by Dimler *et al.* [15], the method achieves Fourier accuracy with Gaussian flexibility. This allows one to tailor the basis in quantum eigenvalue calculations to the underlying classical phase space structure, with the potential for enormous numerical savings. The efficiency of the method relative to the Fourier grid rises steeply with dimensionality, defeating exponential scaling. In the classical limit the method reaches the remarkable efficiency of 1 basis function per 1 eigenstate.

The von Neumann basis set [12] is a subset of the "coherent states" of the form

$$g_{nl}(x) = \left(\frac{2\alpha}{\pi}\right)^{1/4} \exp\left[-\alpha(x - x_n)^2 + i\frac{p_l}{\hbar}(x - x_n)\right] \quad (1)$$

where n and l are integers. Each basis function is a Gaussian centered at $(x_n, p_l) = (na + x_0, \frac{lh}{a} + p_0)$ in phase space, where x_0 and p_0 are arbitrary shifts. The parameter $\alpha = \frac{\sigma_p}{2\sigma_x}$ controls the FWHM of each Gaussian in x and p space. Taking $\Delta x = a$, $\Delta p = h/a$ as the spacing between neighboring Gaussians in x and p space respectively, we note that $\Delta x \Delta p = h$ so we have exactly one basis function per unit cell in phase space. As shown in [13] this implies completeness in the Hilbert space.

The "complete" vN basis, where n and l run over all integers, spans the infinite Hilbert space. In any numerical calculation, however, n and l take on a finite number of values, producing N Gaussian basis functions $\{g_i(x)\}$, $i = 1, ..., N$. Since the size of one vN unit cell is h, the area of the truncated vN lattice is given by $S^{\mathrm{vN}} = Nh$.

The pseudospectral Fourier method (also known as the sinc discrete variable representation [16]) is a widely used tool in quantum simulations [17–20]. In this method a function $\psi(x)$ that is periodic in L and band limited in $K = \frac{P}{\hbar}$ can be written in the following form: $\psi(x) = \sum_{n=1}^{N} \psi(x_n)\theta_n(x)$, where $x_n = \delta_x(n-1)$, and $\delta_x = \frac{\pi\hbar}{P} = \frac{L}{N}$. The basis functions $\{\theta_n(x)\}$ are given by [21]

$$\theta_n(x) = \sum_{j=(-N/2)+1}^{N/2} \frac{1}{\sqrt{LN}} \exp\left[\frac{i2\pi j}{L}(x - x_n)\right], \quad (2)$$

which can be shown to be sinc functions that are periodic on the domain $[0, L]$ [22]. The set $\{\theta_i(x)\}$ $i = 1, .., N$ spans a rectangular shape in phase space with area of $S^{\mathrm{FGH}} = 2LP = 2L\frac{\pi\hbar}{\delta_x} = Nh$. Thus N unit cells in the vN lattice and N grid points in the Fourier-grid Hamiltonian (FGH) method cover the same rectangle with an area in phase space of

$$S^{\mathrm{vN}} = S^{\mathrm{FGH}} = Nh \quad (3)$$

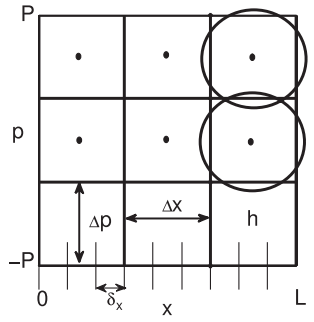

FIG. 1. $N = 9$ coordinate grid points and $N = 9$ vN unit cells span the same area in phase space, $S = Nh$. The vN basis functions are Gaussians located at the center of each unit cell.

(Fig. 1). This suggests that N vN basis functions confined to this area will be equivalent to the Fourier basis set. Unfortunately, the attempt to use N Gaussians as a basis set for the area in Eq. (3) (Fig. 1) is unsuccessful, a consequence of the Gaussians on the edges protruding from the truncated space. However, by combining the Gaussian and the Fourier basis functions we can generate a "Gaussian-like" basis set that is confined to the truncated space. We use the basis sets $\{g_i(x)\}$ and $\{\theta_i(x)\}$ to construct a new basis set, $\{\tilde{g}_i(x)\}$:

$$\tilde{g}_m(x) = \sum_{n=1}^{N} \theta_n(x) g_m(x_n) \tag{4}$$

for $m = 1, \ldots, N$. The new basis set is in some sense, the Gaussian functions with periodic boundary conditions, henceforth, pvN. We can write Eq. (4) in matrix notation as: $\tilde{G} = \Theta G$ where $G_{ij} = g_j(x_i)$. By taking the width parameter $\alpha = \frac{\Delta p}{2\hbar \Delta x}$ we guarantee that the pvN functions have no linear dependence and that the matrix G is invertible, that is $\tilde{G}G^{-1} = \Theta$. The invertibility of G implies that both bases span the same space.

The representation of a state $|\psi\rangle$ in the pvN basis set is given by

$$|\psi\rangle = \sum_{m=1}^{N} |\tilde{g}_m\rangle a_m. \tag{5}$$

Using the completeness relationship for nonorthogonal bases [23], $|\psi\rangle$ can be expressed as

$$|\psi\rangle = \sum_{n=1}^{N} \sum_{m=1}^{N} |\tilde{g}_m\rangle (S^{-1})_{mn} \langle \tilde{g}_n | \psi \rangle. \tag{6}$$

where $S_{ij} = \langle \tilde{g}_i | \tilde{g}_j \rangle = \sum_{n=1}^{N} g_i^*(x_n) g_j(x_n)$ or $S = G^\dagger G$. Comparing with Eq. (5) we find that $a_m = \sum_{n=1}^{N} (S^{-1})_{mn} \langle \tilde{g}_n | \psi \rangle$.

Although the periodic von Neumann (pvN) and the Fourier methods span the same rectangle in phase space, the localized nature of the basis functions in the pvN method can lead to significant advantages. In particular, if $|\psi\rangle$ has an irregular phase space shape we may expect that some of the pvN basis functions will fulfill the relation: $\langle \tilde{g}_j | \psi \rangle = 0$, $j = 1, \ldots, M$. Due to the nonorthogonality of the basis, we cannot simply eliminate the states $\tilde{g}_j$, since the *coefficients* of $\tilde{g}_j$ contain S^{-1} and therefore include contributions from remote basis functions, but we can take advantage of the vanishing overlaps by defining a new basis $\{\tilde{b}_i(x)\}$,

$$|\tilde{b}_i\rangle = \sum_{j=1}^{N} |\tilde{g}_j\rangle (S^{-1})_{ji}, \tag{7}$$

henceforth, the pvb basis (the acronym will be explained below). Equation (7) takes the form $B = GS^{-1} = (G^\dagger)^{-1}$ or $G^\dagger B = \mathbf{1}$ at the Fourier grid points. Inserting Eq. (7) into Eq. (6), $|\psi\rangle$ can be written as

$$|\psi\rangle = \sum_{n=1}^{N} |\tilde{b}_n\rangle c_n = \sum_{n=1}^{N} |\tilde{b}_n\rangle \langle \tilde{g}_n | \psi \rangle. \tag{8}$$

By assumption, M of the coefficients are zero, hence in order to represent $|\psi\rangle$ in this basis set we need only $N' = N - M$ basis functions.

Before turning to the time-independent Schrödinger equation (TISE), we give a brief review of parallel developments in signal processing where the vN representation was discovered independently by Gabor with the role of (p, x) played by (ω, t) [24]. For many years, the nonorthogonal nature of the basis made it difficult to find the expansion coefficients, but in 1980, Bastiaans [25] showed that the coefficients can be calculated by taking the inner product between $|\psi\rangle$ and a set of biorthogonal functions $\{b_i\}$ $\langle \tilde{b} | \psi \rangle$, where $\langle g_j | b_i \rangle = \delta_{ij}$ [cf. Eq. (7)]. Two major problems remained in implementing the Gabor transform. First, in Bastiaans's formalism there is no explicit formula for the $\{b_i\}$ in the general case. Second, as shown by Balian and Low, the Gabor basis is unstable in the sense that even for $|\psi\rangle$ localized in p and x remote Gaussians are needed for the completeness sum [27,28,35]. In practice, an oversampled grid ($\Delta\omega\Delta t < 2\pi$ or $\Delta x \Delta p < h$) is almost always required [4,29,30]. Wexler and Raz developed a discrete version of the Gabor expansion in which a finite number of coefficients is sufficient for a complete representation of a discrete, periodic signal [29]; in fact, their Eq. (23) is identical to our relation $G^\dagger B = \mathbf{1}$ below Eq. (7). However, there is no underlying continuous basis in their approach, and they still found it necessary to oversample in order to achieve localization of the coefficient vector.

The formalism introduced in this Letter contains two central innovations relative to what has previously been done in the von Neumann and Gabor literature. First, our approach is formulated in terms of a continuous basis of the $\{\theta_i\}$ functions [Eq. (4)]. This has several important consequences. It formally ensures the completeness of the pvN basis on a rectangular phase space region, establishing a rigorous equivalence with the discrete Fourier method via Nyquist's theorem. Moreover, the existence

of an underlying continuous basis allows a variety of generalizations. For example leaving the $\{\theta_i\}$ functions unchanged in Eq. (4) but introducing a scaling transformation on the Gaussians by changing $g_m(x_n)$, allows a simple wavelet generalization of our approach [31]. Finally, it allows us to apply the pvN and the pvb bases to the TISE [Eq. (9) and (10) below], something that would not be clear how to do without an underlying continuous basis. The second innovation is the use of the completeness relationship [Eq. (6)], which provides a closed expression for the $\{b_i\}$ that includes S^{-1} explicitly [Eq. (7)]. Equation (7) indicates that while the $\{g_i\}$ are localized the $\{b_i\}$ are not, a point that seems to have been overlooked in the signal processing community [29,32,33]. This motivates the exchange of the roles of the $\{g_i\}$ and $\{b_i\}$ in our approach, an exchange that we show below is crucial to the removal of basis functions and therefore the efficient solution of the TISE. Therefore we call the method "periodic von Neumann with biorthogonal exchange,"or pvb.

We now turn to the formulation of the TISE. The Hamiltonian matrix elements are evaluated as follows:

$$H_{ij}^{\mathrm{pvN}} = \langle \tilde{g}_i|H|\tilde{g}_j\rangle = \sum_{m=1}^{N}\sum_{n=1}^{N} g_i^*(x_m)\langle\theta_m|H|\theta_n\rangle g_j(x_n)$$
$$= \sum_{m=1}^{N}\sum_{n=1}^{N} g_i^*(x_m)H_{mn}^{\mathrm{FGH}} g_j(x_n) \qquad (9)$$

and, similarly,

$$H_{ij}^{\mathrm{pvb}} = \sum_{m=1}^{N}\sum_{n=1}^{N} b_i^*(x_m)H_{mn}^{\mathrm{FGH}} b_j(x_n), \qquad (10)$$

where $H^{\mathrm{FGH}} = V^{\mathrm{FGH}} + T^{\mathrm{FGH}}$ and the potential and the kinetic matrix are given by, $V_{ij}^{\mathrm{FGH}} \approx V(x_i)\delta_{ij}$ and

$$T_{ij}^{\mathrm{FGH}} = \frac{\hbar^2}{2M}\begin{cases} \frac{K^2}{3}\left(1+\frac{2}{N^2}\right), & \text{if } i=j \\ \frac{2K^2}{N^2}\frac{(-1)^{j-i}}{\sin^2(\pi\frac{j-i}{N})}, & \text{if } i\neq j \end{cases} \qquad (11)$$

[34]. The eigenvalue problem in a nonorthogonal basis set becomes $HU = sUE$; in the pvN basis set s is given by $G^\dagger G$ and in the pvb basis set s is given by

$$B^\dagger B = S^{-1}G^\dagger G S^{-1} = S^{-1}. \qquad (12)$$

Diagonalization should give accurate results for all wave functions localized to the classically allowed region of the rectangle. Note that in the multidimensional implementation, the S^{-1} matrix required in Eq. (9) can be constructed separately for each dimension. As a result, the computational effort to construct the pvb basis set is negligible compared with diagonalizing the Hamiltonian.

As a numerical test of the pvN basis set we studied the standard example of the harmonic oscillator $V(x) = \frac{m\omega^2x^2}{2}$ in units such that $m = \hbar = \omega = 1$. We calculated the seventh excited energy using different number of pvN and conventional Gaussian basis functions. In the Gaussian basis set, the Hamiltonian and the overlap matrices were calculated analytically as $H_{ij} = \langle g_i|H|g_j\rangle = \int_{-\infty}^{\infty} g_i^*(x)[-\frac{d^2}{dx^2} + V(x)]g_j(x)dx$ and $S_{ij} = \langle g_i|g_j\rangle = \int_{-\infty}^{\infty} g_i^*(x)g_j(x)dx$. The results, shown in Fig. 2(a), show that the pvN basis set can provide many (14) orders of magnitude more accuracy than the standard Gaussian basis set. In fact, the results obtained with the pvN basis set are exactly as accurate as in the Fourier grid method. Calculation of the kinetic energy spectrum (not shown) shows that the pvN has a perfect quadratic dependence, exactly as in the Fourier grid method. while the vN spectrum is highly flawed.

We now turn to the removal of basis functions. Figure 2(b) shows results for the Morse potential, $V(x) = D(1-e^{-\beta x})^2$, with $D = 12$, $m = 6$, $\beta = 0.5$ and $\hbar = 1$. To obtain 12 digits of accuracy in the bound state energies, the Fourier grid Hamiltonian (FGH) method required 400 grid points between $[-2.5, 60.1]$ and the pvN method 20×20 pvN functions with $\alpha = 0.3191$. Despite the extreme accuracy of the pvN basis, removing even a single basis function from the rectangular phase space area introduces large errors [Fig. 2(b)]. The method is even more sensitive to removal of basis functions than the Fourier grid method. In contrast, in the pvb basis set we are able to remove a large fraction of the basis functions and construct much lower dimensional H^{pvb} and S^{pvb} matrices without losing significant accuracy. Figure 3(a) shows the phase space interpretation: although it requires 400 Fourier grid basis functions to span the rectangular area in phase space, in the pvb basis we can suffice with just the basis functions centered in the classically allowed region (magenta squares).

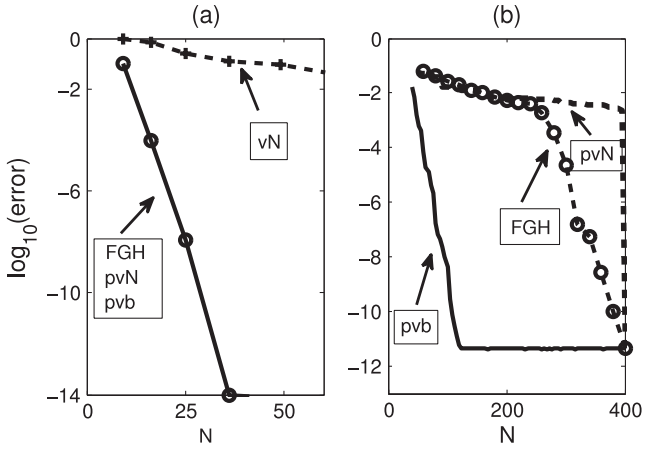

FIG. 2. (a) Error in the 7th eigenvalue of the harmonic oscillator for a rectangular phase space grid as a function of the basis set size N. The pvN, pvb, and Fourier grid methods all give identical results (solid), 14 orders of magnitude more accurate than the usual vN basis (dashed). (b) Error in the 24th eigenvalue of the Morse potential as one discards basis functions from a rectangular phase space lattice. The pvb (dashed), pvN (solid) and Fourier grid (dotted) behave completely differently.

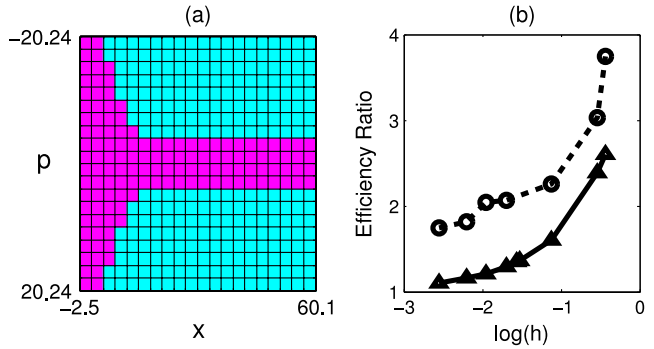

FIG. 3 (color online). (a). Phase space area spanned in the pvb method (magenta) and in the pvN (or FGH) method (full rectangle) for Morse. (b) Efficiency ratio (defined as number of basis functions per converged eigenstates) of the pvb (solid) and FGH (dashed) methods for the Morse potential as function of $\hbar$.

The ability to localize a pvb function at a specific point in phase space results in the remarkable concept of 1 basis function per 1 eigenstate. This means that in order to calculate N eigenenergies we need only N basis functions. Obviously, such one per one efficiency, if reachable, will be the ideal efficiency for any basis set. In order to test the ability of the pvb method to reach the ideal efficiency we examined the Morse potential and looked for the smallest basis that provides 12 digits of accuracy for all the eigenvalues up to $E = 11.25$. The pvb method indeed tends to the ideal efficiency in the classical limit $\hbar \to 0$ [Fig. 3(b)]. This remarkable result is unique for methods based on phase space localization [26].

The true power of the method is in the application to higher dimensional systems. As an illustration, consider the potential $V(r, \theta) = (1 - \exp(-\alpha(\theta)r^2))^2$ where $\alpha = ((1 - \cos(3\theta))/4)^2 + 0.05$. This threefold symmetric potential (Fig. 4), which is a realistic model for a system of three identical particles and fixed hyperradius, is quite challenging for the FGH method. Taking $m = 96$, $\hbar = 1$ gives 760 states below $E = 0.996$. In order to get two digits of accuracy for all those states, one needs ~11 000 FGH grid points, while with the pvb basis set convergence is achieved with only 1500 basis functions. For higher accuracy (four digits), the FGH breaks down completely while the pvb method requires fewer than 3000 basis functions [Figs. 5(a) and 5(b)]. Figure 5(c) shows again that as $\hbar \to 0$ the efficiency tends to 1 basis function per 1 eigenstate (because of the size of the calculations we consider just 3 digits of accuracy). In contrast, the FGH efficiency as $\hbar \to 0$ is determined by the ratio between the classical phase space and the box that contains it, which we calculate to be ~10 for this system using Monte Carlo integration. Note that in going from 1-d to 2-d, the savings provided by the pvb relative to the FGH method has gone from 2 to 7–10 for qualitatively similarly potentials. This suggests that the relative efficiency of the pvb method increases rapidly with dimension.

To explore the scaling with dimensionality more fully, consider a harmonic oscillator with 1-d classical phase space volume v up to energy E. For the D-dimensional oscillator, the total phase space volume up to energy E is $V = v^D/D!$ In the classical limit, the total number of states is determined by V/h^D and therefore in this limit the efficiency of pvb relative to FGH is determined by the ratio of the phase space volumes spanned. Defining a to be the area of the box surrounding the 1-d oscillator phase space, the volume of the box surrounding the D-dimensional phase space is $A = a^D$ and the ratio of phase space volumes is $S = V/A = s^D/D!$, where $s = v/a = \pi/4$ for the harmonic oscillator. For the Morse, Coulomb, and other chemically relevant potentials, the 1D ratio $s < \pi/4$ and the D-dimensional phase space volume scales more slowly than $v^D/D!$ [22]; these effects combine so that the relative efficiency of the pvb method rises steeply with dimension. As a result of the $D!$ in the expression for V, the method remarkably defeats

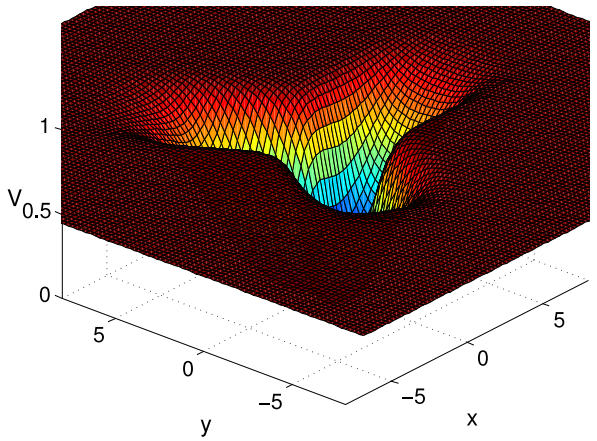

FIG. 4 (color online). The triangle potential: a two dimensional test case for the pvb method.

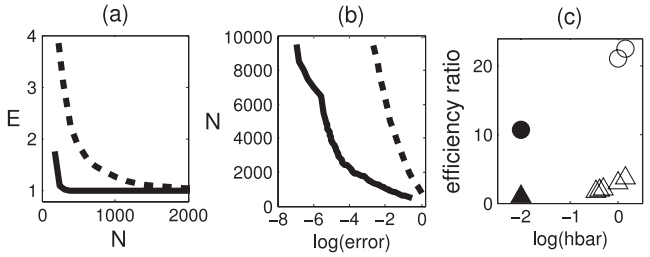

FIG. 5. Triangle potential results for pvb(solid) and FGH (dashed) (a) The calculated highest eigenenergy E as a function of basis set size N. (b) The accuracy of the calculated highest eigenenergy as a function of basis set size N. (c) Efficiency ratio of the pvb (△) and FGH (○) methods as a function of $\hbar$. The ▲ (pvb) and ● (FGH) signify that the value is an approximation to the $\hbar \to 0$ value, given by the ratio between the size of the phase space spanned by the basis and the classical phase space.

exponential scaling. A more detailed analysis [22] shows that for $D \gg v/h = g$ the method scales polynomially: $V = D^g/g!$.

Work in progress includes application to vibrational eigenvalue calculations for realistic polyatomic molecules, electronic eigenvalues for multielectron atoms, and extension of the approach to the time-dependent Schrödinger equation.

This work was supported by the Israel Science Foundation and made possible, in part, by the historic generosity of the Harold Perlman family. We thank Bill Poirier for helpful discussions.

[1] R. Kosloff, in *Numerical Grid Methods and their Application to Schrödinger's Equation*, edited by C. Cerjan (Kluwer, Boston, 1993).
[2] C. C. Marston and G. G. Balint-Kurti, J. Chem. Phys. **91**, 3571 (1989).
[3] G. W. Wei, J. Phys. B **33**, 343 (2000).
[4] M. J. Davis and E. J. Heller, J. Chem. Phys. **71**, 3383 (1979).
[5] I. P. Hamilton and J. C. Light, J. Chem. Phys. **84**, 306 (1986).
[6] Z. Bačić, R. M. Whitnell, D. Brown, and J. C. Light, Comput. Phys. Commun. **51**, 35 (1988).
[7] S. Garashchuk and J. C. Light, J. Chem. Phys. **114**, 3929 (2001).
[8] E. T. Whittaker, Proc. R. Soc. Edinburgh, Sect. A **35**, 181 (1915).
[9] H. Nyquist, Trans. AIEE 1 **47**, 617 (1928).
[10] C. E. Shannon, Proc. IRE **37**, 10 (1949).
[11] S. Fechner, F. Dimler, T. Brixner, G. Gerber, and D. J. Tannor, Opt. Express **15**, 15387 (2007).
[12] J. von Neumann, Math. Ann. **104**, 570 (1931).
[13] A. M. Perelomov, Theor. Math. Phys. **6**, 156 (1971).
[14] B. Poirier and A. Salam, J. Chem. Phys. **121**, 1690 (2004).
[15] F. Dimler, S. Fechner, A. Rodenberg, T. Brixner, and D. J. Tannor, New J. Phys. **11**, 105052 (2009).
[16] D. T. Colbert and William H. Miller, J. Chem. Phys. **96**, 1982 (1992).
[17] J. Dai and J. C. Light, J. Chem. Phys. **107**, 1676 (1997).
[18] A. J. H. M. Meijer and E. M. Goldfield, J. Chem. Phys. **108**, 5404 (1998).
[19] X. T. Wu, A. B. McCoy, and E. F. Hayes, J. Chem. Phys. **110**, 2354 (1999) (2002).
[20] J. H. Baraban, A. R. Beck, A. H. Steeves, J. F. Stanton, and R. W. Field, J. Chem. Phys. **134**, 244311 (2011).
[21] D. J. Tannor, *Introduction to Quantum Mechanics: A Time-dependent Perspective* (University Science Books, Sausalito, 2007), p. 163; see Eq. (11).
[22] See Supplemental Material at http://link.aps.org/supplemental/10.1103/PhysRevLett.109.070402 for details.
[23] D. J. Tannor, *Introduction to Quantum Mechanics: A Time-dependent Perspective* (University Science Books, Sausalito, 2007), p. 118; see Eq. (8).
[24] D. Gabor, J. Am. Inst. Electr. Eng. **93**, 429 (1946).
[25] M. J. Bastiaans, Proc. IEEE **68**, 538 (1980).
[26] R. Lombardini and B. Poirier, Phys. Rev. E **74**, 036705 (2006).
[27] I. Daubechies, IEEE Trans. Inf. Theory **36**, 961 (1990).
[28] R. Balian, C R Acad Bulg Sci. III **292**, 1357 (1981).
[29] J. Wexler and S. Raz, Signal Processing **21**, 207 (1990).
[30] S. Qian and D. Chen, IEEE Trans. Signal Process. **41**, 2429 (1993).
[31] A. Shimshovitz and D. J. Tannor (to be published).
[32] J. G. Daugman, IEEE Trans. Acoust. Speech Signal Process. **36**, 1169 (1988).
[33] M. Porat and Y. Y. Zeevi, IEEE Trans. Pattern Anal. Mach. Intell. **10**, 452 (1988).
[34] D. J. Tannor, *Introduction to Quantum Mechanics: A Time-dependent Perspective* (University Science Books, Sausalito, CA, 2007), p. 172; see Eq. (11).
[35] F. Low, in *A Passion for Physics—Essays in Honor of Geoffrey Chew* (World Scientific, Singapore, 1985), p. 17.